

Decay of kaonium in a chiral approach

S. P. Klevansky[†] and R. H. Lemmer[‡]

*Institut für Theoretische Physik, Universität Heidelberg,
Philosophenweg 19, 69120 Heidelberg, Germany.*

(Dated: February 24, 2024)

Abstract

The decay of the K^+K^- -hadronic atom kaonium is investigated non-perturbatively using meson-meson interaction amplitudes taken from leading order chiral perturbation theory in an approach adapted from that proposed by Oller and Oset [18]. The Kudryavtsev-Popov eigenvalue equation is solved numerically for the energy shift and decay width due to strong interactions in the $1s$ state. These calculations introduce a cutoff ~ 1.4 GeV in $O(4)$ momentum space that is necessary to regulate divergent loop contributions to the meson-meson scattering amplitudes in the strong-interaction sector. One finds lifetimes of $(2.2 \pm 0.9) \times 10^{-18}$ s for the ground state of kaonium.

PACS numbers: 11.10.St, 11.30.Rd, 13.75.Lb

[†]Corresponding author: S. P. Klevansky

Electronic address: spk@physik.uni-heidelberg.de

[‡] Permanent address: School of Physics, University of the Witwatersrand, Johannesburg,
Private Bag 3, WITS 2050, South Africa.

Electronic address: rh_lemmer@mweb.co.za

1. Introduction

As is the case for the hadronic atoms ponium [1] and kaonic hydrogen [2] the energy shifts and decay widths in the coulomb spectrum of the hadronic atom K^+K^- , or kaonium [3], also depend primarily on the scattering length of the interacting particles, in this case K^+ and K^- . This scattering length, in turn, is determined by the properties of the $K\bar{K}$ strong interactions and the associated models for the possible structures of the $f_0(980)$ and $a_0(980)$ scalar mesons. These proposals include a kaon–antikaon molecular bound state [4–11], a $q^2\bar{q}^2$ state [12], or a $q\bar{q}$ state [13–17].

The molecular state option has been explored in some detail in [6, 8–11]. These calculations all employ a $SU_V(3) \times SU_A(3)$ symmetric model Lagrangian density [6] to generate meson–meson interaction vertices via vector meson exchange. A rather different route was followed by Oller and Oset [18]. These authors take the meson–meson interaction vertices from leading order chiral perturbation theory (χ PT) as being an appropriate theoretical realization of low energy QCD [19], and solve the resulting Lippmann–Schwinger equation for the corresponding T -matrix elements to provide a non-perturbative description of meson–meson scattering and reactions. This approach introduces one additional parameter insofar as the meson loops occurring in the resulting equations need to be regularized with a high-momentum cutoff. Using a three-momentum cutoff of ~ 1 GeV they find good agreement with the measured $\pi\pi \rightarrow \pi\pi$ phase shifts and $\pi\pi \rightarrow K\bar{K}$ inelasticities up to center-of-mass (c.m.) collision energies of order $\sqrt{s} \sim 1.2$ GeV. The masses and decay widths of the $f_0(980)$ and $a_0(980)$ scalar mesons are also satisfactorily reproduced as complex poles of the relevant T matrices.

In the following we adapt the Oller–Oset [18] approach to study the energy shifts and decay widths introduced by the strong interactions into the spectrum of kaonium.

2. Non-perturbative χ PT scattering amplitudes

The calculations reported in [18] start from the χ PT leading order interaction Lagrangian density [18, 20, 21] \mathcal{L}_2 for the pseudoscalar meson octet at low energies to generate tree-level chirally symmetric meson–meson interaction amplitudes, or 4-point vertices, of good isospin I for s -wave meson scattering. The explicit form of \mathcal{L}_2 is given by Eq. (17) of the Appendix. These vertices form a symmetric matrix V_{ij}^I , where the labels i and j each refer to the channels $\{K\bar{K}\}$, $\{\pi\pi\}$ or $\{\pi^0\eta\}$. (We retain the labelling convention of [18] by setting $(i, j) = (1, 2)$ where 1 refers to $\{K\bar{K}\}$ for both $I = 0$ and 1, while 2 refers to $\{\pi\pi\}$ for $I = 0$ or $\{\pi^0\eta\}$ for $I = 1$).

Knowing the V_{ij}^I one can construct the coupled integral equations for the associated scattering matrices T_{ij}^I . However, for s -wave scattering an important simplification occurs. As argued in [18], one can then replace the V_{ij}^I , which are in general off-shell, by their on-shell values which only depend on the square of the total c.m. energy $s = P_0^2$, provided that at the same time one uses the physical values of the pion decay constant $f \rightarrow f_\pi \approx 93$ MeV and the meson masses $(m_\pi, m_K, m_\eta) \approx (140, 496, 547)$ MeV that enter into the calculations. Then the coupled integral equations for T_{ij}^I are replaced by algebraic equations that can be solved analytically. In particular, one obtains $T_{11}^I(s)$ for $K\bar{K}$ in both isospin channels by first “dressing” the bare $K\bar{K}$ interaction $V_{11}^I(s)$ with $\pi\pi$ or $\pi^0\eta$ polarization loops $\Pi_{22}^I(s) = \Pi_{\pi\pi}(s)$ or $\Pi_{\pi^0\eta}(s)$ for $I = 0$ or 1 respectively, and then inserting this dressed interaction into

the Lippmann–Schwinger equation for $T_{11}^I(s)$ to find the result already quoted in [18],

$$T_{11}^I(s) = \frac{(1 - V_{22}^I \Pi_{22}^I) V_{11}^I + V_{12}^I \Pi_{22}^I V_{21}^I}{(1 - V_{11}^I \Pi_{11}^I)(1 - V_{22}^I \Pi_{22}^I) - V_{12}^I \Pi_{22}^I V_{21}^I \Pi_{11}^I} \quad (1)$$

Here $\Pi_{11}^I(s) = \Pi_{K\bar{K}}(s)$ accounts for the common $K\bar{K}$ polarization loop in both isospin channels.

We characterize the various meson loop diagrams appearing in $T_{11}^I(s)$ by the common symbol $-i\Pi(s)$ where

$$\Pi(s) = -i\epsilon \int \frac{d^4l}{(2\pi^4)} \frac{1}{(l^2 - m_a^2)} \frac{1}{(l + P_0)^2 - m_b^2}, \quad s = P_0^2 \quad (2)$$

that involves the integral over the two meson propagators of masses (m_a, m_b) in the loop; ϵ is a symmetry factor [22] that takes on the values $(1/2, 1)$ depending on whether $m_a = m_b$ refer to identical mesons or not. Since this integral diverges for large 4-momenta, we introduce a cut-off Λ in $O(4)$ momentum space. The on-shell versions of the $V_{ij}^I(s)$ together with the regulated, closed form expressions for $\Pi(s)$ from which $\Pi_{\pi\pi}(s)$, $\Pi_{\pi^0\eta}(s)$ and $\Pi_{K\bar{K}}(s)$ may be constructed, are listed as Eqs. (20), (21) and (23) in the Appendix.

The poles of $T_{11}^I(s)$ on the appropriate sheet of the cut complex s plane are identified [18] with the masses and half widths of the scalars $f_0(600)$ (or σ) and $f_0(980)$ for $I = 0$, and $a_0(980)$ for $I = 1$. This sheet structure depends in turn on the analytic behaviour of the functions $\Pi(s)$ in the denominator of Eq. (1) that develop unitarity cuts along the real s -axis, starting at the production thresholds of $\pi\pi$, $\pi^0\eta$ and $K\bar{K}$ mesons at $s = (m_a + m_b)^2 = 4m_\pi^2$, $(m_{\pi^0} + m_\eta)^2$ or $4m_K^2$ respectively. The prescription for analytically continuing $T_{11}^I(s)$ through these cuts onto the relevant Riemann sheet in the lower half plane where these poles lie is detailed in [18].

Using this information together with the closed forms for polarization functions and interaction vertices assembled in the Appendix, we reconstruct the $f_0(980)$ pole of $T_{11}^0(s)$ as a function of the cutoff in the $O(4)$ regularization scheme. The results are given in Fig. 1 that displays the width Γ_{f_0} versus the mass M_{f_0} , parametrized by Λ in order to illustrate their sensitivity to cutoff. These calculations assume a Breit–Wigner form $\sim (P_0 - M_{f_0} + i\Gamma_{f_0}/2)^{-1}$ with $P_0 = \sqrt{s}$ for $T_{11}^0(s)$ in the vicinity of the pole. We use these results to fix Λ by requiring that the real part of the pole coincide with the observed $f_0(980)$ mass as quoted in either the PDG [23] data tables, $[(980 \pm 10) - i(20 \text{ to } 50)]$ MeV, or the Fermilab E791 experiment [24] that gives $[(975 \pm 3) - i(22 \pm 2)]$ MeV. Then

$$M_{f_0} - \frac{i}{2}\Gamma_{f_0} = [(980 \pm 10) - i(23 \text{ } ^{-7}_{+5})] \text{ MeV} \quad \text{for} \quad \Lambda = 1.35^{+0.19}_{-0.16} \text{ GeV} \quad (3)$$

in the first case, while

$$M_{f_0} - \frac{i}{2}\Gamma_{f_0} = [(975 \pm 3) - i(26 \mp 2)] \text{ MeV} \quad \text{for} \quad \Lambda = 1.43 \mp 0.05 \text{ GeV}. \quad (4)$$

in the second. These choices for Λ also reproduce the observed $f_0(980)$ half-widths rather satisfactorily. Taken together, this suggests that the appropriate values of the cutoff Λ in the $O(4)$ regularization scheme should lie within a relatively small window around 1.4 GeV.

3. Scattering lengths

The associated $K\bar{K}$ scattering lengths of good isospin are given in terms of the $T_{11}^I(s)$ by the standard expression [22]

$$a_{K\bar{K}}^I = - \lim_{s \rightarrow 4m_K^2} \frac{T_{11}^I(s)}{8\pi\sqrt{s}} = - \frac{T_{11}^I(4m_K^2)}{16\pi m_K} \quad (5)$$

The scattering lengths $a_{K\bar{K}}^I$ are complex numbers with $\text{Im } a_{K\bar{K}}^I < 0$ because of the presence of the open $\pi\pi$ and $\pi^0\eta$ decay channels for $I = 0$ and $I = 1$. One finds, in units of the inverse kaon mass m_K^{-1} , that

$$a_{K\bar{K}}^0 = 3.530 - 2.077i, \quad a_{K\bar{K}}^1 = 1.651 - 1.416i, \quad \Lambda = 1.35 \text{ GeV} \quad (6)$$

or

$$a_{K\bar{K}}^0 = 3.303 - 1.713i, \quad a_{K\bar{K}}^1 = 1.655 - 1.221i, \quad \Lambda = 1.43 \text{ GeV} \quad (7)$$

for the two Λ 's found in Eqs. (3) and (4).

The values calculated above for the isoscalar scattering length are similar in order of magnitude and sign to early direct experimental measurements [25] that yield $a_{K\bar{K}}^0 = [(3.13 \pm 0.30) - (0.67 \pm 0.07)i]m_K^{-1}$, and a later analysis [26] of $\pi\pi$ data that gives $a_{K\bar{K}}^0 = (4.36 - 1.49i)m_K^{-1}$. No similar measurements are available for $a_{K\bar{K}}^1$. A model-dependent estimate [27] extracted from more recent $pp \rightarrow dK^+\bar{K}^0$ data [28] yields $a_{K\bar{K}}^1 \approx [-(0.05 \pm 0.05) - i(1.59 \pm 0.60)]m_K^{-1}$. These numbers may also be compared with the rough estimate $a_{K\bar{K}}^0 \sim a_{K\bar{K}}^1 \sim (2.98 - 2.13i)m_K^{-1}$ from the zero-range universal approximation [29] $M - \frac{i}{2}\Gamma \approx 2m_K - m_K^{-1}(a_{K\bar{K}}^I)^{-2}$ for common meson masses and half-widths $\sim (980 - 35i)$ MeV in both isospin channels.

Moving from T -matrices labelled by good isospin to particle-antiparticle labels with the aid of Eq. (18), one obtains the common strong interaction scattering lengths for the physical K^+K^- and $K^0\bar{K}^0$ channels as

$$a_{K^+K^-} = a_{K^0\bar{K}^0} = \frac{1}{2}(a_{K\bar{K}}^0 + a_{K\bar{K}}^1) = 2.591 - 1.747i \quad \text{or} \quad 2.479 - 1.467i \quad (8)$$

for cutoffs (1.35, 1.43) GeV respectively, if the K^0K^+ mass difference $\Delta = m_{K^0} - m_{K^\pm} \approx 4$ MeV is ignored. If not, then the K^+K^- scattering length becomes [30]

$$a_p = \left(\frac{a_{K^+K^-} - k_0 a_{K\bar{K}}^0 a_{K\bar{K}}^1}{1 - k_0 a_{K^+K^-}} \right) = 2.688 - 1.896i \quad \text{or} \quad 2.567 - 1.566i \quad (9)$$

for the two cutoffs in question. Here $k_0 = \sqrt{2m_{K^0}\Delta}$.

4. Strong interaction energy shifts and decay widths of kaonium

The level shifts and decay widths for kaonium due to strong interactions have been discussed in detail in [8, 11] using the vector meson exchange model Lagrangian density [6] mentioned in the Introduction. We re-evaluate these quantities using the basic χ PT \mathcal{L}_2 density given by Eq. (17) instead.

The unshifted ground state of kaonium lies at $E_{1s} = -\frac{1}{2}\alpha^2\mu = -6.576$ keV where $\mu = \frac{1}{2}m_{K^\pm}$ is the reduced mass with $m_{K^\pm} = 494$ MeV and $\alpha \approx 1/137$. Contrary to the case of pionium, however, where charge exchange $\pi^+\pi^- \rightarrow \pi^0\pi^0$ dominates the decay [1], $K^+K^- \rightarrow K^0\bar{K}^0$ is not allowed due the K^0K^\pm mass difference. Thus the principal strong decay modes are kaonium $\rightarrow \pi\pi + \pi^0\eta$ that proceed via strange quark annihilation.

Isospin is broken by the coulomb field as well as the meson mass difference. Since the binding energy of kaonium is small relative to that of the strongly interacting $K\bar{K}$ ground state of $f_0(980)$ at ~ 10 MeV, the modified energy spectrum can be found by the standard procedure [31] of joining the zero momentum s -wave scattering function of mixed isospin $u(r) = r\psi(r) \rightarrow 1 - r/a_p$ of the pair emerging from the strong interaction zone with scattering length a_p , onto an exponentially decaying pure coulomb wave at infinity. This is given by an incoming Whittaker function [32] $W_{i\eta, 1/2}(2ikr)$ at complex momentum $k = k_\lambda = -i\mu\alpha\lambda$ with $\text{Re}\lambda > 0$. The coulomb parameter index for attractive fields then reads $i\eta = -i\mu\alpha/k = 1/\lambda$. Here $\lambda = \lambda_n$, $n = 1, 2, \dots$ is a set of eigenvalues to be determined by the logarithmic matching condition at $r = d$ outside the strong interaction zone of extent $\sim 1/m_K$. One thus retrieves the Kudryavtsev–Popov eigenvalue equation [33] which we rearrange as

$$\alpha_{pc} = 2\mu\alpha\left[\frac{\lambda_n}{2} + \ln \lambda_n + \psi\left(1 - \frac{1}{\lambda_n}\right) + \gamma\right], \quad n = 1, 2, \dots \quad (10)$$

Here ψ is the standard digamma function [32], $\gamma = 0.57721\dots$ the Euler constant and $\alpha_{pc} = 1/a_{pc}$ is the physical K^+K^- inverse scattering length in the presence coulomb interactions as defined by Bethe [31],

$$\alpha_{pc} = \alpha_p - 2\mu\alpha[\ln(2\mu\alpha d) + \gamma] \quad (11)$$

with $\alpha_p = 1/a_p$ from Eq. (9). The role of α_{pc} as the relevant experimental observable has also been stressed in [34]. We estimate $d \approx 2.2m_K^{-1}$ for the (calculable) Bethe joining radius [31] for the coulomb plus strong interaction field; d is thus fixed and not a parameter. Since d is much smaller than the Bohr radius $1/\mu\alpha$ of kaonium, the small argument approximation for $W_{i\eta, 1/2}(2ikr)$ suffices for deriving Eq. (10).

The revised s -wave energy levels and decay widths (λ_n is complex because α_p and therefore α_{pc} is complex) of the kaonium atom are given by

$$E_{\lambda_n} - \frac{i}{2}\Gamma_{\lambda_n} = \frac{(k_{\lambda_n})^2}{2\mu} = -\frac{1}{2}\alpha^2\lambda_n^2\mu \quad (12)$$

In the absence of any strong interactions $a_p \rightarrow 0$ so that $\alpha_{pc} \rightarrow \infty$. From Eq. (10) this means that λ_n is then determined by the poles of $\psi(1 - \frac{1}{\lambda_n})$ as $\lambda_n^{-1} = n$, and one recovers the pure coulomb spectrum from Eq. (12).

The input for α_{pc} on the left hand side of Eq. (10) is obtained from Eqs. (9) and (11) as

$$\alpha_{pc} = (2.589 - 1.654i)^{-1}m_K \quad \text{or} \quad (2.459 - 1.375i)^{-1}m_K \quad (13)$$

for $\Lambda = 1.35$ or 1.43 GeV respectively. Eq. (10) has multiple roots. Solving for the eigenvalue λ_1 corresponding to the $1s$ ground state of kaonium, one finds $\lambda_1 = 0.9812 + 0.0118i$ or $\lambda_1 = 0.9822 + 0.0098i$ for the above two values of the cutoff. The energy shifts $\Delta E_{1s} = (E_{\lambda_1} - E_{1s})$, half-widths $\frac{1}{2}\Gamma_{1s} = \frac{1}{2}\Gamma_{\lambda_1}$ and resulting lifetimes $\tau_{1s} = \hbar/\Gamma_{1s}$ (in units 10^{-18}s) introduced by the strong interactions are then [42]

$$\begin{aligned}
\Delta E_{1s} - \frac{i}{2}\Gamma_{1s} &= [(246_{-25}^{+21}) - \frac{i}{2}(304_{-88}^{+194})] \text{ eV}, \quad \tau_{1s} = 2.2 \mp 0.9, \quad \Lambda = 1.35_{+0.16}^{-0.19} \text{ GeV} \\
&= [(233_{-7}^{+8}) - \frac{i}{2}(254_{-24}^{+28})] \text{ eV}, \quad \tau_{1s} = 2.6 \mp 0.3, \quad \Lambda = 1.43 \mp 0.05 \text{ GeV}
\end{aligned} \tag{14}$$

Notice that the energy shifts are repulsive and of the same order of magnitude as the decay widths.

The uncertainties on Λ have been also included in these calculations. The larger error bars at the lower cutoff clearly overlap with those at the upper cutoff. A conservative estimate for the lifetime is thus provided by the spread of values at the lower cutoff of $\tau_{1s} \sim 1$ to $3 \times 10^{-18}\text{s}$, rounded to the nearest integer.

Fig. 2 gives a parametric plot of Γ_{1s} versus ΔE_{1s} for a range of Λ 's. The inset in this figure shows an analogous plot of the quantities $-Im a_{pc}$ versus $Re a_{pc}$ that provide the input for generating the main curve. One sees that the two curves behave in a similar fashion, and moreover turn at approximately the same value $\Lambda = 1.18 \text{ GeV}$ where $Re a_{pc}$ reaches its maximum value in the inset of Fig. 2. This behavior is confirmed by the original Deser *et al.* approximate formula [35] that is recovered by expanding the roots of Eq. (10) to lowest order in the interaction parameter $2\mu\alpha a_{pc}$ about their limiting values $\lambda_n^{-1} = n$. Then

$$\Delta E_{1s} - \frac{i}{2}\Gamma_{1s} \approx 2\mu^2\alpha^3 a_{pc} = \frac{2\pi}{\mu} a_{pc} |\psi_{1s}(0)|^2 \tag{15}$$

for the $1s$ ground state, where $\psi_{1s}(0) = (\mu\alpha)^{3/2}\pi^{-1/2}$. In this limit one sees that the two parametric curves in Fig. 2 are related by a simple rescaling of their axes.

The Deser estimate, Eq. (15) gives

$$\begin{aligned}
\Delta E_{1s} - \frac{i}{2}\Gamma_{1s} &\approx [(248_{-19}^{+19}) - \frac{i}{2}(318_{-94}^{+202})] \text{ eV}, \quad \tau_{1s} = 2.1 \mp 0.9, \quad \Lambda = 1.35_{+0.16}^{-0.19} \text{ GeV} \\
&\approx [(236_{-7}^{+7}) - \frac{i}{2}(264_{-26}^{+30})] \text{ eV}, \quad \tau_{1s} = 2.5 \mp 0.3, \quad \Lambda = 1.43 \mp 0.05 \text{ GeV}
\end{aligned} \tag{16}$$

for the energy shift and width in the place of Eq. (14). In the present instance this approximation is seen to be fairly reliable, overestimating the energy shifts and widths by $\sim 1\%$ and $\sim 5\%$ respectively, when compared with the eigenvalue solutions obtained from the Kudryavtsev–Popov equation.

5. Summary and conclusions

We have studied the energy shift and decay width of the $1s$ ground state of kaonium using interactions taken from chiral perturbation theory to construct the strong $K\bar{K}$ scattering amplitudes. These calculations contain a single regulating cutoff Λ that is fixed by requiring that the relevant pole of the $K\bar{K}$ scattering amplitude in the isoscalar channel reproduce the experimental $f_0(980)$ mass determinations within their quoted error bars [23, 24].

The calculated decay lifetimes for kaonium then range from ~ 1 to 3×10^{-18} s. Direct experimental information on the energy shift and decay width of kaonium is not yet available. However, such experiments have already been performed in the case of kaonic hydrogen (K^-p) by the DEAR collaboration [36]. These data have been analyzed using a variety of theoretical approaches to extract scattering lengths, see for example [2, 37, 38].

A similar experimental program for kaonium would allow one to extract a value for the physical K^+K^- scattering length a_{pc} by combining Eqs. (12) and (10) to determine a value for λ_1 and hence α_{pc} . This information would also allow a re-assessment of the various theoretical models mentioned in the Introduction for the $f_0(980)$ and $a_0(980)$ scalar mesons by comparing with their predictions for the strong scattering lengths $a_{K\bar{K}}^I$ and hence a_{pc} . The additional feature [39] that kaonium is the only purely mesonic atom with hidden strangeness that decays via strangeness annihilation makes such experimental and theoretical investigations of particular interest.

Indirect methods of observation of the formation and decay of kaonium [3, 40, 41] may also be feasible in the future.

Acknowledgments

One of us (RHL) would like to thank the Ernest Oppenheimer Memorial Trust for research support in the form of a Harry Oppenheimer Fellowship. The kind hospitality of the Institut für Theoretische Physik, Universität Heidelberg, is also gratefully acknowledged. We would also like to thank A. Gal for bringing the second reference included in [30] to our attention.

6. Appendix

(i) Lagrangian density \mathcal{L}_2 and the 4-point interaction vertices

The leading order χ PT interaction Lagrangian density for the pseudoscalar meson octet used in [18] is

$$\mathcal{L}_2 = \frac{1}{12f^2} \text{Tr}((\partial_\mu \Phi \Phi - \Phi \partial_\mu \Phi)^2 + M \Phi^4) \quad (17)$$

where

$$\Phi = \begin{pmatrix} \frac{1}{\sqrt{2}}\pi^0 + \frac{1}{\sqrt{6}}\eta & \pi^+ & K^+ \\ \pi^- & -\frac{1}{\sqrt{2}}\pi^0 + \frac{1}{\sqrt{6}}\eta & K^0 \\ K^- & \bar{K}^0 & -\frac{2}{\sqrt{6}}\eta \end{pmatrix}$$

is a 3×3 matrix of the meson fields in $SU(3)$ flavor space constructed from the Gell-Mann λ matrices that are the generators of this group; η is identified with η_8 . M is the diagonal mass matrix $M = \text{diag}(m_\pi^2, m_\pi^2, 2m_K^2 - m_\pi^2)$ and f is the pion decay constant. The trace runs over the $SU(3)$ flavor space.

Call $iV_{ij}^I(s)$ the set of 4-point vertex diagrams generated by $i\mathcal{L}_2$. Working in a set of basis states of good isospin

$$|(K\bar{K})^{0,1}\rangle = -\frac{1}{\sqrt{2}}[K^+K^- \pm K^0\bar{K}^0] \quad (18)$$

and

$$|(\pi\pi)^0\rangle = -\frac{1}{\sqrt{3}}[\pi^+\pi^- + \pi^-\pi^+ + \pi^0\pi^0], \quad |(\pi^0\eta)^1\rangle = \pi^0\eta \quad (19)$$

the on-shell values [43] for the V_{ij}^I are

$$\begin{aligned} V_{11}^0 &= \frac{3}{4}\frac{s}{f^2}, \quad V_{21}^0 = \frac{1}{2}\sqrt{\frac{3}{2}}\frac{s}{f^2}, \quad V_{22}^0 = \frac{1}{f^2}(2s - m_\pi^2) \\ V_{11}^1 &= \frac{1}{4}\frac{s}{f^2}, \quad V_{21}^1 = -\sqrt{\frac{2}{3}}\frac{1}{f^2}\left(\frac{3}{4}s - \frac{1}{12}m_\pi^2 - \frac{1}{4}m_\eta^2 - \frac{2}{3}m_K^2\right), \quad V_{22}^1 = \frac{1}{3}\frac{m_\pi^2}{f^2} \end{aligned} \quad (20)$$

Here \sqrt{s} is the total collisional energy in the CM system.

(ii) *Polarization loop integrals*

The expression for the $O(4)$ regularized integral in Eq. (2) depends on where s lies relative to the cut that starts at the branch point $(m_a + m_b)^2$. For $s > (m_a + m_b)^2$ on the upper lip of the cut along the real axis, the integral acquires an imaginary part and one finds

$$\Pi(s) = \frac{\epsilon}{(4\pi)^2} \left[\frac{m_a^2}{m_a^2 - m_b^2} \ln\left(1 + \frac{\Lambda^2}{m_a^2}\right) - \frac{m_b^2}{m_a^2 - m_b^2} \ln\left(1 + \frac{\Lambda^2}{m_b^2}\right) - L_{ab}(s) \right] \quad (21)$$

with $L_{ab}(s)$ given by

$$\begin{aligned} L_{ab}(s) &= -1 - \frac{1}{2} \left(\frac{m_a^2 + m_b^2}{m_a^2 - m_b^2} - \frac{m_a^2 - m_b^2}{s} \right) \ln \frac{m_a^2}{m_b^2} \\ &+ \sqrt{f_{ab}} \left[\tanh^{-1} \left(\frac{\sqrt{f_{ab}}}{1 - \frac{m_a^2 - m_b^2}{s}} \right) + \tanh^{-1} \left(\frac{\sqrt{f_{ab}}}{1 + \frac{m_a^2 - m_b^2}{s}} \right) \right] - i\pi\sqrt{f_{ab}}, \quad s > (m_a + m_b)^2 \\ \sqrt{f_{ab}} &= \left(1 - \frac{(m_a - m_b)^2}{s} \right)^{1/2} \left(1 - \frac{(m_a + m_b)^2}{s} \right)^{1/2} = \frac{2p_{ab}}{\sqrt{s}} \end{aligned} \quad (22)$$

and p_{ab} is the magnitude of the 3-momentum of either meson in the c.m. system. Note that all expressions are symmetric under the interchange $m_a \rightarrow m_b$. Equation (21) with $m_a = m_\pi$ and $m_b = m_\eta$ gives the closed form for $\Pi_{\pi^0\eta}(s)$.

For equal masses $m_a = m_b = m$, $\Pi(s)$ reduces to the simple form

$$\begin{aligned} \Pi(s) &= \frac{\epsilon}{(4\pi)^2} \left[1 + \ln\left(1 + \frac{\Lambda^2}{m^2}\right) + \frac{m^2}{\Lambda^2} \left(1 + \frac{m^2}{\Lambda^2}\right)^{-1} - 2\sqrt{f} \tanh^{-1} \sqrt{f} + i\pi\sqrt{f} \right], \quad s > 4m^2 \\ \sqrt{f} &= \left(1 - \frac{4m^2}{s} \right)^{1/2} \end{aligned} \quad (23)$$

Setting $m = m_\pi$ or m_K with $\epsilon = 1/2$ or 1 respectively then leads to closed forms for $\Pi_{\pi\pi}(s)$ and $\Pi_{K\bar{K}}(s)$.

References

- [1] For recent reviews, see J. Gasser, V.E. Lyubovitskij, and A. Rusetsky, Phys. Rept. **456**, (2008) 167; Ann. Rev. Nucl. Part. Sci. **59**, (2009) 169.
- [2] Ulf-G. Meißner, U. Raha and A. Rusetsky, Eur. Phys. J. C **35**, (2004) 349.
- [3] S. Wycech and A. M. Green, Nucl. Phys. A **562**, (1993) 446.
- [4] J. Weinstein and N. Isgur, Phys. Rev. Lett. **48**, (1982) 659; Phys. Rev. D **27**, (1983) 588; D **41**, (1990) 2236.
- [5] T. Barnes, Phys. Lett. B **165**, (1985) 434.
- [6] D. Lohse, J. W. Durso, K. Holinde and J. Speth, Nucl. Phys. A **516**, (1990) 513; G. Janßen, B. C. Pearce, K. Holinde and J. Speth, Phys. Rev. D **52**, (1995) 2690.
- [7] J. A. Oller, Nucl. Phys. A **714**, (2003) 161.
- [8] S. Krewald, R. H. Lemmer and F. P. Sassen, Phys. Rev. D **69**, (2004) 016003.
- [9] Y.-J. Zhang, H.-C. Chiang, P.-N. Shen, and B.-S. Zou, Phys. Rev. D **74**, (2006) 014013.
- [10] T. Branz, T. Gutsche and V.E. Lyubovitskij, Eur. Phys. J. A **37**, (2008) 303.
- [11] R. H. Lemmer, Phys. Rev. C **80**, (2009) 045205.
- [12] N. N. Achasov and V. N. Ivanchenko, Nucl. Phys. B **315**, (1989) 465.
- [13] L. Montanet, Nucl. Phys. B (Proc. Suppl.) **86**, (2000) 381; V.V. Anisovich *et al.*, Phys. Lett. B **480**, (2000) 19.
- [14] N. A. Tornquist and M. Roos, Phys. Rev. Lett. **76**, (1996) 1575.
- [15] V. Dmitrasinović, Phys. Rev. C **53**, (1996) 1383.
- [16] R. Delbourgo and M. D. Scadron, Int. J. Mod. Phys. A **13**, (1998) 657.
- [17] M. D. Scadron, G. Rupp, F. Kleefeld, and E. van Beveren, Phys. Rev. D **69**, (2004) 014010; Erratum, Phys. Rev. D **69**, (2004) 059901.
- [18] J. A. Oller and E. Oset, Nucl. Phys. A **620**, (1997) 438; Erratum, Nucl. Phys. A **652**, (1997) 407.
- [19] J. Gasser and H. Leutwyler, Ann. Phys. **158**, (1984) 142.
- [20] J. Gasser and H. Leutwyler, Nucl. Phys. B **250**, (1985) 465.
- [21] G. Ecker, Prog. Part. Nucl. Phys. **35**, (1995) 1.
- [22] J. L. Peterson, Phys. Rep. **C 2**, (1971) 158.
- [23] K. Nakamura *et al.* (Particle Data Group) JPG **37**, (2010) 075021.
- [24] Fermilab E791 Collaboration, E. M. Aitala *et al.*, Phys. Rev. Lett. **86**, (2001) 765.
- [25] W. W. Wetzel *et al.*, Nucl. Phys. B **115**, (1976) 208.
- [26] R. Kamiński and L. Leśniak, Phys. Rev. C **51**, (1995) 2264.
- [27] R. H. Lemmer, Phys. Lett. B **633**, (2006) 265.
- [28] V. Kleber, *et al.*, Phys. Rev. Lett. **91**, (2003) 172304.
- [29] E. Braaten and M. Kusunoki, Phys. Rev. D **69** (2004) 074005; M. B. Voloshin, Phys. Lett. B **579** (2004) 316.
- [30] A. D. Martin and G. G. Ross, Nucl. Phys. B **16**, (1970) 479; R. H. Dalitz and S. F. Tuan, Ann. Phys. **8** (1959) 100.
- [31] H. A. Bethe, Phys. Rev. **76**, (1949) 38; J. D. Jackson and J. M. Blatt, Rev. Mod. Phys. **22**, (1950) 77.
- [32] M. Abramowitz and I. A. Stegun, Editors, *Handbook of Mathematical Functions* (Dover Pub-

- lications, Inc., New York, 1965).
- [33] A.E. Kudryavtsev and V. S. Popov, JETP Lett. **29**, 280 (1979); V. S. Popov, A.E. Kudryavtsev, and V. D. Mur, Sov. Phys. JETP **50**, 865 (1979).
 - [34] B. Holstein, Phys. Rev. D **60**, (1999) 114030.
 - [35] S. Deser, M. L. Goldberger, K. Baumann, and W. Thirring, Phys. Rev. **96**, (1954) 774; T. L. Trueman, Nucl. Phys. **26**, (1961) 57.
 - [36] M. Cargnelli *et. al* [DEAR collaboration], in Proceedings of "HadAtom" Workshop, 13–17 October 2003, ECT* (Trento, Italy), arXiv:hep-ph/0401204; *ibid.* Int. J. Mod. Phys. A **20**, (2005); G Beer *et al.*, [DEAR collaboration] Phys. Rev. Lett. **94**, (2005) 212302.
 - [37] B. Borasoy, R. Nißler, and W. Weise, Phys. Rev. Lett. **94**, (2005) 213401.
 - [38] B. Borasoy, U.-G. Meißner, and R. Nißler, Phys. Rev. C **74**, (2006) 055201.
 - [39] H. Poth, Invited paper, Workshop on Physics at Lear with Low–Energy Cooled Antiprotons, 9–16 May 1982, Erice, Sicily, CERN–EP/82–82, 24 June 1982.
 - [40] B. Kerbikov, Z. Phys. A **353**, (1995) 113.
 - [41] S. V. Bashinsky and B. Kerbikov, Phys. Atm. Nucl. **59**, (1996) 1979.
 - [42] It is interesting to note that these shifts and widths, which have been generated using chiral interaction amplitudes, are bracketed by those based on local [8] or non–local [11] model potentials to describe the strong interactions.
 - [43] Note that since the pions act as identical bosons in this basis, some authors e.g. [6, 18], include an additional normalization of $1/\sqrt{2}$ in the definition of $|(\pi\pi)^0\rangle$. Hence the matrix elements V_{ij}^0 given in Eq. (20) are larger by a factor $\sqrt{2}$ than those listed by Oller and Oset for each pion label 2 appearing on the matrix.

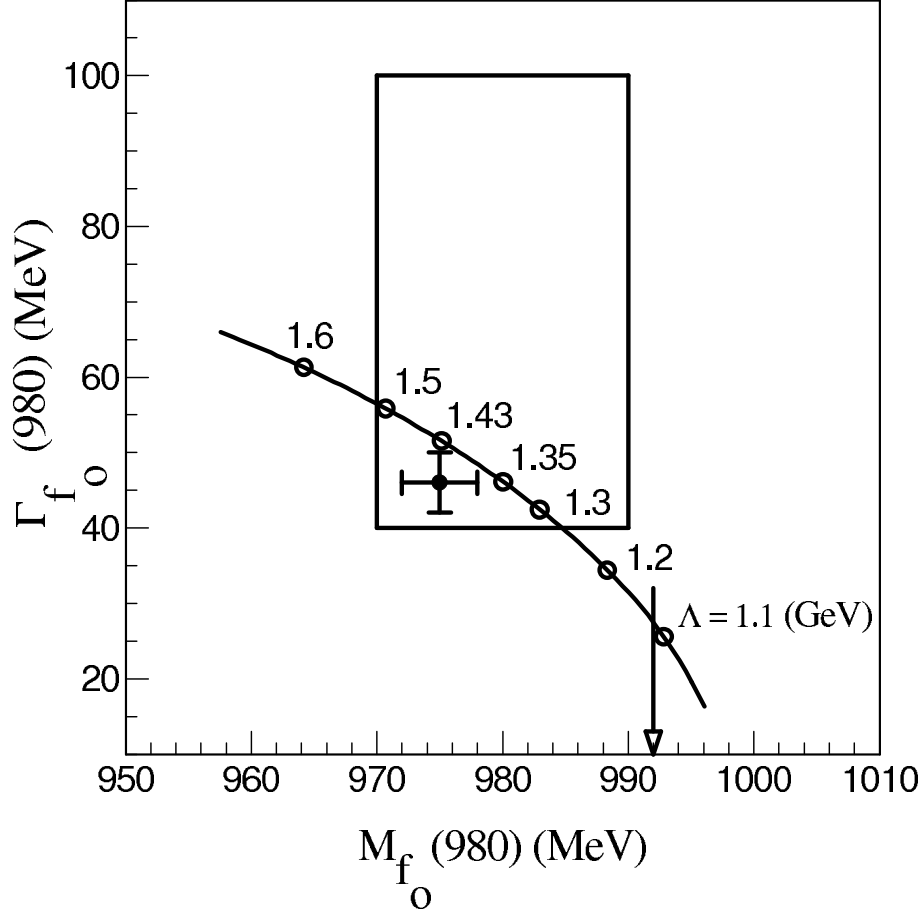


FIG. 1: Mass-width relation for $f_0(980)$ parametrized by the $O(4)$ cutoff Λ . The rectangle gives the limits on M_{f_0} and Γ_{f_0} suggested in the PDG data listings [23], while the cross indicates the Fermilab E791 measurements [24] and the associated error bars. The $K\bar{K}$ threshold at $2m_K \approx 992$ MeV is indicated by the arrow. The physical parameters used in this evaluation are $(m_\pi, m_K, f_\pi) = (140, 496, 93)$ in MeV.

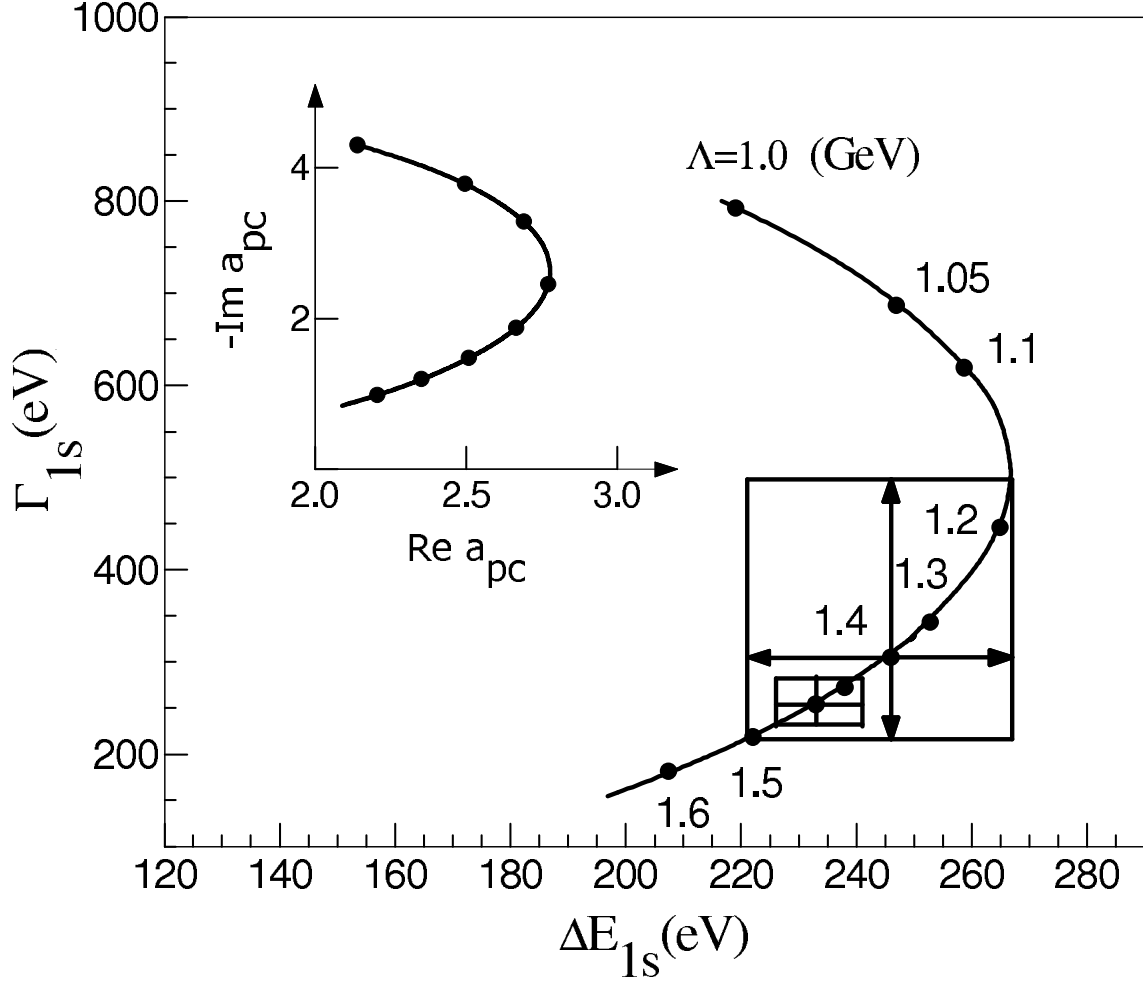


FIG. 2: The $1s$ decay width Γ_{1s} versus energy shift ΔE_{1s} for kaonium parametrized by the $O(4)$ cutoff Λ . The estimated energy shift and corresponding width can lie anywhere along the arc of the curve intersecting the calculated uncertainties-on- Λ rectangles centered at $\Lambda = 1.35$ or 1.43 GeV (large and small rectangles) respectively. These rectangles correspond to fitting either the PDG [23] or the Fermilab E791 data [24] for the observed $f_0(980)$ mass within the experimental uncertainties, refer Fig. 1. The inset shows the $-\text{Im } a_{pc}$ versus $\text{Re } a_{pc}$ parametric curve in units m_K^{-1} calculated for the same set of Λ 's. The shape of this curve mimics that of the width-shift curve. The latter also turns in the close vicinity of $\Lambda = 1.18$ GeV where the parametric a_{pc} curve turns as $\text{Re } a_{pc}$ reaches its maximum value in the inset.